



MINERAL DISTRIBUTION IN THE LUNAR SOUTH POLE-AITKEN BASIN DERIVED FROM SELENE MULTIBAND IMAGER

K. Uemoto^{1,4}, M.Ohtake¹, J. Haruyama¹, T. Matsunaga², Y. Yokota², T. Morota¹, R. Nakamura³, S. Yamamoto², and T. Iwata¹

¹Japan Aerospace Exploration Agency (JAXA), ²National Institute for Environmental Studies (NIES),

³National Institute of Advanced Industrial Science and Technology (AIST), ⁴The University of Tokyo

Introduction: SPA is one of the biggest basin (2500 km in diameter [1]) on the lunar farside. It has been suggested, in previous studies, that most of the upper crustal material of this basin was excavated and the lower crust or mantle materials are exposed [e.g., 2]. Therefore anorthosite which consist of upper crust possibly ejected from the basin, and particularly, this excavation effects is the most significant at the central part of the basin [1]. However, Pieters et al. [2] reported that there is anorthosite in the small crater south of the Alder crater (77 km in diameter). This crater locates within estimated transient cavity of the SPA basin [2]. Additionally, Ohtake et al. [3] reported that the purest anorthosite (>98 vol.% plagioclase) exposed in the Leibnitz crater which located in the northwest of the Alder crater [3] (Figure 1).

If rocks of purest anorthosite composition present within SPA in many locates these presences suggest following possibly; (1) anorthosite was generated by differentiation of the impact melt, (2) anorthosite was remained without being ejected, or (3) anorthosite was collapsed down from outside of the transient cavity.

In this study, we analyzed craters within SPA and investigated distribution of purest anorthosite. Especially, we focused craters at the lower elevation areas of the SPA because these locations supposed to excavate deepest location within the crust.

Methods: We chose the craters to analyze by selecting higher reflectance locations because the reflectance of anorthosite is higher than the rocks with more mafic rich compositions based on the Clementine 750 nm-base map. The craters we analyzed are Antoniadi, Alder, Apollo, Bose, Bellingsgauzen, Hopmann, Minnaert, Numerov, Lemaitre, Poincare, Zeeman, Buffon, Cori, Crommelin, Cabannes, Eijkman, Fizeau, Riedel, Vallis Plank, Schrodinger, AlderSrim, ApolloW, Bose, and AntoniadiW. They are 15-143 km in diameter (Figure 1 and Table 1).

We used images taken by the SELENE Multiband Imager (MI) to investigate the mineralogy within the craters and their surrounding area in the SPA basin. The reflectance spectra in the standard viewing geometry were calculated by using the photometric function proposed by digital terrain models (DTMs) generated by the MI. MI has both visible and near-infrared coverages with spectral bands at 415, 750, 900, 950, and 1000 nm on VIS sensor, and 1000, 1050, 1250 and 1550 nm

on NIR sensor. In all MI images, spatial resolution is adjusted as 20 m x 20 m per pixel. At each location, the reflectance is given by averaging an area corresponding to 6 x 6 pixels in the MI VIS to remove spatial variation. We also made the color-composite image (Figure 2a). In this image, red, green and blue are assigned to a continuum-removed absorption depth at 950, 1050 and 1250 nm, respectively. These approximately indicate the relative strengths of pyroxene, olivine, and plagioclase absorptions, respectively.

We estimated the mineralogy by using absorption band generated by plagioclase (around 1250 nm), olivine (around 1050 nm) and pyroxene (around 1000 nm). Presence of the purest anorthosite is determined by the biggest absorption depth around 1250 nm.

Additionally, we checked and confirmed that the purest anorthosite are exposed at fresh surface by comparing maturity map generated by using an expression of OMAT by Lucey et al. [4].

Results: In the crater of Poincare NE, we found the purest anorthosite in the wall (Figures 2 and 3). In the maturity map, locations of the purest anorthosite are fresh surfaced areas. Possibly they were generated by falling down of the crater wall. However, on the crater of Antoniadi, Alder, Bellingsgauzen, Hopmann, Minnaert, Numerov, Lemaitre and Zeeman, there are no evidence the purest anorthosite. In these craters pyroxene is a most abundant minerals because of showing that the absorptions deepest at 950 nm.

Discussion: By these results, we found that the purest anorthosite (>98 vol.% plagioclase) is exists in the inner part of the transient cavity than previously studies. From these results and the distribution of anorthosite in SPA basin, we consider that these anorthosites were differentiated from the impact melt or remained without being ejected by the impact.

There are craters which we do not still analyze in SPA basin, so the more study is required. Then, we grasp the distribution of other minerals. And we draw the map of the distribution of mineral and rock types on the SPA basin.

References: [1] Spudis P.D. et al. (1994) *Science*, 266, 1848-1851. [2] Pieters C.M. et al. (2001) *JGR*, 106, 28,001-28,022. [3] Ohtake M. et al. (2009) *Nature*, 461, 236-401. [4] Lucey P. et al. (2000) *JGR*, 105, 20, 377-20, 386. [5] Hiesinger H. and Head J.W. (2004) *LPSC XXXV*, Abstract #1164.

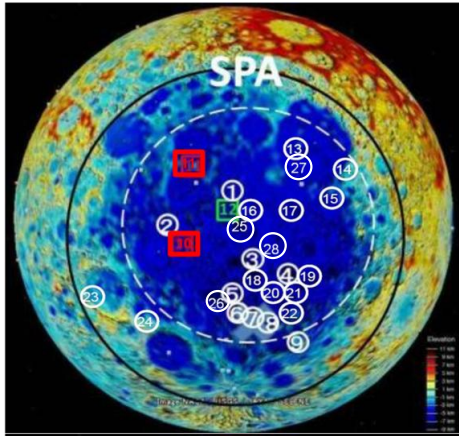


Figure 1. Distribution of the craters we analyzed in this study. Elevation map is from www.google.com/moon/. Large black circle is rim of SPA from Spudis et al. [1]. White dotted line circle is transient crater by Hiesinger et al. [5]. Numbers of each location correspond to the crater numbers in Table 1. Red squares indicate locations purest anorthosite (>98 vol.% plagioclase) was found. White circles are designated places where no purest anorthosite was found. Green square indicates the place where anorthosite was reported in previous study [2].

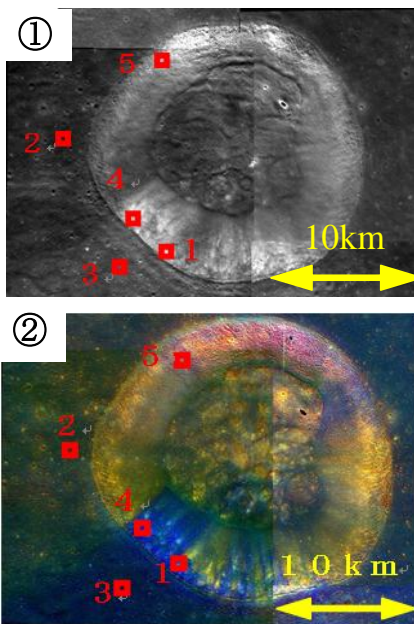


Figure 2. ① Multiband Imager 750 nm image of Poincare NE. ② Color-composite image of Poincare NE. Red, green, and blue are assigned to a continuum-removed absorption depth at 950, 1050, and 1250 nm. These approximately indicate the relative strengths of pyroxene, olivine, and plagioclase absorptions, respectively. Reflectance spectra of red squares is presented in Fig. 3. Squares 1 and 4 indicate locates purest anorthosite was found. Squares 2, 3, 5, 6, and 7 indicate locations it was not found.

CraterName	latitude	longitude	diameter(km)	PurestAnorthosite
1 AlderN	42S	181W	15	No
2 Hopmann	51S	180E	88	No
3 Bellinsgauzen	61S	164W	20	No
4 LemaîtreW	62S	155W	8	No
5 MinnaertNE	64S	175W	20	No
6 Antoniadi	70S	168W	143	No
7 NumerovE	70S	154W	40	No
8 NumerovC	70S	163W	113	No
9 ZeemanN	70S	137W	30	No
10 PoincaréNE	53S	161E	20	Yes
11 (Leipnitz)	47S	178W	77	Yes
12 (Alder)	38S	181W	245	(Yes)*
13 ApolloWa	35S	157W	334	No
14 BuffonSW	41S	134W	3	No
15 RidelW	48S	142W	42	No
16 AlderS	49S	177W	75	No
17 CoriE	50S	150W	56	No
18 Cabannes	61S	170W	73	No
19 FizeauW	58S	137W	96	No
20 Lemaître	61S	149W	86	No
21 EijkmanE	62S	137W	50	No
22 Crommelin	68S	147W	88	No
23 VallisPlanckW	58S	122E	43	No
24 Schrodinger	66S	128E	35	No
25 AlderSrim	50S	177W	75	No
26 AntoniadiWrim	68S	177W	143	No
27 ApolloWb	36S	155W	7	No
28 BoseW	54S	170W	4	No

Table.1 The list of the craters we analyzed
*The result of Alder (12) is not purest anorthosite but simply 'anorthosite' because of the data from Clementine.

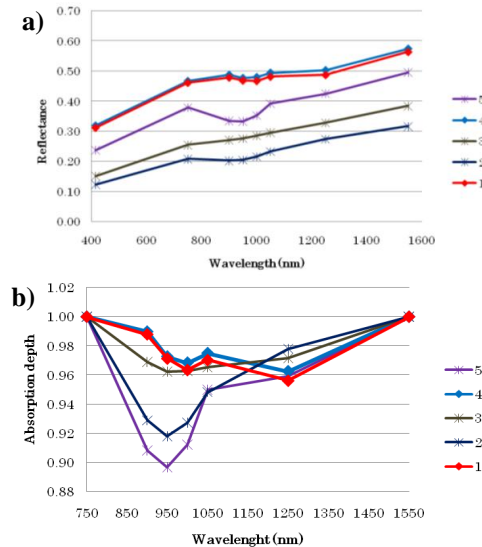


Figure 3. Reflectance spectrum of each locations North crater of the PoincareNE. a) is representative reflectance spectra of PoincareNE crater. b) is absorption after continuum removal spectra number 1 and 4 indicate largest absorption about 1250 nm indicating purest anorthosite composition.

Graphs of red (1) and blue (4) in both profiles indicate that the purest anorthosite is present. Other color graphs (2, 3, and 5) indicate that it is not present.

At each location, the reflectance is given by averaging an area corresponding to 6 x 6 pixels in the MI VIS to remove spatial variation.